

Fig. 4 Effect of wing sweep and thickness on $C_{L\alpha}$.

18% as much volume as the large balance housing body), and this resulted in only a 3% increase in L/D_{\max} , which is believed to be well within the accuracy of the data. Note that L/D_{\max} exhibited a nearly linear decay as thickness ratio was increased logarithmically. For the more slender wings, the models with 80° sweep angles obtained the higher values of L/D_{\max} for a particular thickness ratio. Optimum sweep angle is more readily obtained from Fig. 3, which indicates that as thickness ratio increased from a value of zero the optimum sweep angle for maximum lift-drag ratio decreased from an angle of 80° or slightly larger to 70° or less for the more blunt shapes tested. The peak in L/D_{\max} for each constant bluntness curve suggests that, as sweep decreases from 90°, the increased lifting surface more than offsets the increase in drag initially, whereas at sweep angles less than optimum, the converse is true. Unfortunately, the angle-of-attack range did not permit many of the more blunt wings to obtain a maximum lift-drag ratio, and the optimum sweep angle for the more blunt bodies could not be definitely ascertained. Newtonian theory, which is shown as calculated, neglecting viscous effects for wings without bodies,² is seen in Fig. 2 to give good prediction of maximum lift-drag ratio for the thickest wings and is useful in determining the optimum sweep angle for these wings (solid symbols on Fig. 3†).

$C_{L\alpha}$ was found to vary linearly or near linearly with thickness ratio as shown in Fig. 4. As sweep angle increased, $C_{L\alpha}$ was seen to decrease, a trend previously obtained on slender wings at lower hypersonic speeds.³ Because the presence of balance housing bodies would tend to introduce negative lift at and near zero degrees angle of attack, the only values of $C_{L\alpha}$ presented are those for wings that had no balance housing bodies, which were the more blunt wings. Within the limitation of the data in Fig. 4, values of $C_{L\alpha}$ for arbitrary combinations of thickness ratio and sweep angle may easily be interpolated.

Of primary concern, of course, is the marked effect of even small degrees of leading edge blunting on L/D_{\max} . It is clear then that the achievement of high L/D_{\max} during reentry (of as much as 4 or more, say) for practical configurations will require the application of much effort and ingenuity on the part of designers.

† As a point of interest, Newtonian theory in a modified form was used, applying a stagnation pressure coefficient given by

$$[(\gamma + 3)/(\gamma + 1)]\{1 - [2/(\gamma + 3)](1/M^2)\}$$

on the cylindrical leading edge section and the spherical segment nose sections and applying $(\gamma + 1)$ to the flat-plate portion of the wings, but it was found that classical Newtonian theory ($C_{p_{\max}} = 2$) generally gave better predictions of all forces and moments.

References

- 1 Arrington, J. P., Joiner, R. C., Jr., and Henderson, A., Jr., "Longitudinal characteristics of several configurations at hypersonic Mach numbers in conical and contoured nozzles," NASA TN D-2489 (1964).
- 2 Olstad, W. B., "Theoretical evaluation of hypersonic forces, moments and stability derivatives for combinations of flat plates, including effects of blunt leading edges, by Newtonian impact theory," NASA TN D-1015 (1962).
- 3 Bertram, M. H. and McCauley, W. C., "Investigation of the aerodynamic characteristics at high supersonic Mach numbers of a family of delta wings having double-wedge sections with the maximum thickness at 0.18 chord," NACA TM L54G28 (1954).

Further Similarity Solutions of Axisymmetric Wakes and Jets

MARTIN H. STEIGER* AND MARTIN H. BLOOM†
Polytechnic Institute of Brooklyn, Freeport, N. Y.

Nomenclature

ρ	= density
μ	= viscosity
h	= static enthalpy
H	= $(h + u^2/2)$ total enthalpy
x, y	= streamwise and radial coordinates with velocity components u and v

Subscripts

e	= conditions at the edge of the viscous layer
x, y	= partial differentiation
0	= conditions along the x axis

THE similarity equation¹⁻³

$$[\eta(F'/\eta)']' + F(F'/\eta)' + \beta\eta[1 - (F'/\eta)^2] = 0 \quad (1a)$$

subject to the boundary conditions

$$F = (F'/\eta)' = 0 \quad \text{at} \quad \eta = 0 \quad (1b)$$

$$F'/\eta = 1.0 \quad \text{as} \quad \eta \rightarrow \infty$$

describes incompressible axisymmetric free-mixing with streamwise pressure gradients, and admits large velocity defects, where the axis velocity ratio u_0/u_e is constant.

Solutions of Eqs. (1) have been presented² for $\beta = 1.0$, and for the range³ $-0.5 < \beta < 0$. For $\beta = 1.0$, it has been shown² that $F' = \eta(1 - 3 \exp - \eta^2/4)$.

This note describes an extension to compressible flow which applies rigorously if the density ratio ρ_e/ρ can be only a function of the similarity variable η . However, it appears that ρ_e/ρ can be represented by a function of η alone only as an approximation when $(u_e^2/2h_e)[1 - (u/u_e)^2]$ is negligible with respect to unity, or when $u_e^2/2h_e$ is constant. Thus when $(u_e^2/2h_e)[1 - (u/u_e)^2] \ll 1$, the isoenergetic compressible equation reduces to the forementioned incompressible form. Exact and integral method solutions of Eqs. (1) in the ranges $-1.0 < \beta < -0.5$ and $0.5 < \beta < 4.0$ are presented herein.

Received September 18, 1964. The study was supported by the Air Force Office of Scientific Research Grant No. AF-AFOSR-1-63. The authors wish to acknowledge the assistance of Karl Chen, who carried out the numerical calculations.

* Assistant Professor, Aerospace Engineering. Member AIAA.

† Professor of Aerospace Engineering and Head of Department of Aerospace Engineering and Applied Mechanics. Associate Fellow Member AIAA.

The governing boundary-layer equations are assumed to be

Continuity

$$(\rho u y)_x + (\rho v y)_y = 0 \quad (2a)$$

Momentum

$$\rho u u_x + \rho v u_y = y^{-1}(\mu y u_y)_y + \rho_e u_e u_{ex} \quad (2b)$$

Total Energy

$$\rho u H_x + \rho v H_y = y^{-1}(\mu y H_y)_y \quad (3a)$$

or alternatively, in terms of static enthalpy,

$$\rho u h_x + \rho v h_y = y^{-1}(\mu y h_y)_y - \rho_e u_e u_{ex} u \quad (3b)$$

State

$$\rho_e/\rho = h/h_e \quad (4)$$

The boundary conditions considered are

$$y = 0 \quad v = u_y = 0 \quad h_y = 0 \quad H_y = 0 \quad (5a)$$

$$y \rightarrow \infty \quad u = u_e(x) \quad (5b)$$

$$h = h_e(x) \quad H = H_e = \text{const}$$

By introducing the similarity functions and variables

$$u = u_e(s) [F'(\eta)/\eta] \quad (6a)$$

$$H = H_e g(\eta) \quad (6b)$$

$$h = h_e(s) G(\eta) \quad (6c)$$

$$s = \int_0^x \mu_e dx \quad (7a)$$

$$\frac{\eta^2}{2} = \left(u_e \int_0^y \rho y dy \right) / s \quad (7b)$$

into Eqs. (2-4), the momentum and energy equations reduce to

$$[CJ(F'/\eta)']' + F(F'/\eta)' + \beta\eta[\varphi - (F'/\eta)^2] = 0 \quad (8a)$$

$$[CJ\varphi']' + F\varphi' = -\xi(u_e^2/2h_e)CJ[(F'/\eta)']^2 \quad (8b)$$

where, if $\varphi = g$, then $\beta = (2s/u_e)(du_e/ds)(H_e/h_e)$ and $\xi = 0$, or if $\varphi = G$, then $\beta = (2s/u_e)(du_e/ds)$ and $\xi = 1.0$. Also,

$$C = \rho\mu/\rho_e\mu_e \quad (9a)$$

$$J = \frac{2}{\eta} \int_0^\eta \frac{\rho_e}{\rho} \eta d\eta \quad (9b)$$

The transformed momentum Eq. (8a) is similar if $C = C(\eta)$, $\beta = \text{const}$, and ρ_e/ρ (which appears in the parameter J) is a function of η alone. The first two conditions are readily

Table 1 Values of u_0/u_e

β	Exact	Integral method
∞	-4.00000	-3.00000
10	-3.47436	-2.81818
5	-3.21401	-2.66667
3	-2.92277	-2.50000
1	-2.00000	-2.00000
0.7	-1.63182	-1.82353
0.5	-1.00000	-1.66667
0	0	-1.0000
-0.1	-0.3493	-0.7778
-0.2	-0.2288	-0.5000
-0.3	0.0002	-0.1429
-0.4	0.3774	0.3333
-0.5	1.0000	1.0000
-0.6	2.0745	2.0000
-0.7	4.103	3.667
-0.8	8.590	7.000
-0.9	23.095	17.000
-1.0	∞	∞

Fig. 1a Axis velocity u_0/u_e vs pressure gradient parameter β , for $\beta \leq 0$.

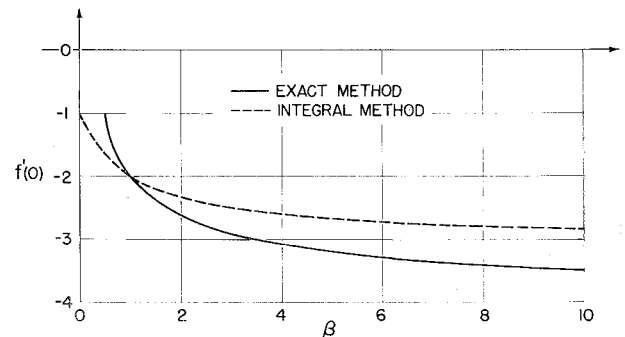
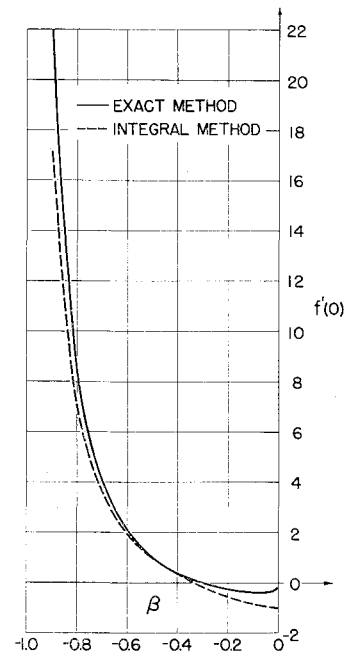


Fig. 1b Axis velocity u_0/u_e vs pressure gradient parameter β , for $\beta \geq 0.5$.

satisfied. It is reasonable to assume $\rho\mu = \rho_e\mu_e$, therefore $C = 1$. The requirement $\beta = \text{const}$ prescribes the variation of u_e . It remains to be shown under what conditions the density ratio is a function of η only.

The density ratio may be expressed alternatively as

$$\rho_e/\rho = g + (u_e^2/2h_e)[g - (F'/\eta)^2] \quad (10a)$$

or

$$\rho_e/\rho = G \quad (10b)$$

If Eq. (10a) is used, then ρ_e/ρ , a function of η , requires $u_e^2/2h_e[g - (F'/\eta)^2] \ll g$, or else $u_e^2/2h_e = \text{const}$. The former restriction is acceptable, for example, if $u_e^2/2h_e \rightarrow 0$ (low speed flow) or if $[g - (F'/\eta)^2] \rightarrow 0$ (i.e., as $\beta \rightarrow -0.5$). On the other hand, the constancy of $u_e^2/2h_e$ implies $\beta = 0$ and leads to a trivial solution of Eq. (8a). However, if $u_e^2/2h_e$ is a slowly varying function of s , the approximation of local similarity may be useful. In this case, local values of $u_e^2/2h_e$ are used in (10a) and local values of β in Eq. (8a).

Furthermore, it is noted that the only solution to the total energy equation which satisfies the boundary conditions (5a) and (5b) is $H = H_e$, and therefore g in the foregoing paragraph and in Eq. (10) should be replaced by unity. This solution corresponds to isenergetic flows.

If expression (10b) is used for the density ratio, then the requirement $J = J(\eta)$ reduces to the possible similar solutions of G , which can be derived from Eq. (8b) with $\varphi = G$ and $\xi = 1$. Nontrivial solutions of Eq. (8b) exist only if $u_e^2/2h_e$

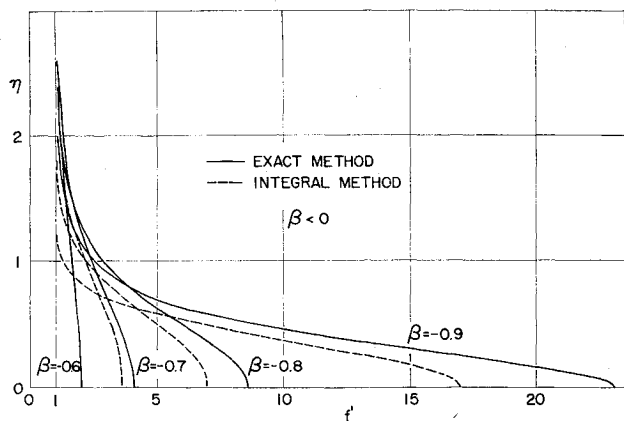


Fig. 2 Velocity profiles for $-1.0 < \beta < -0.5$.

$\neq 0$. However, the factor $u_e^2/2h_e$ is generally a function of s and therefore prevents rigorous similarity of G . Locally similar approximate solutions also may be useful in this case.

The remainder of this note is concerned with flows wherein $u_e^2/2h_e[1 - (F'/\eta)^2] \ll 1.0$. With this condition, $J = \eta$ and Eq. (8a) reduces to Eq. (1), with $\beta = (2s/u_e)(du_e/ds)(H_e/h_e)$. Solutions of Eqs. (1) have been obtained by numerical integration (utilizing an IBM 7040 digital computer) and by a momentum integral method. The computer program is analogous to the one discussed in Ref. 4.

Direct integration of (1a), with (1b) and $(F'/\eta)_{\infty} = 0$, yields

$$\int_0^{\infty} \frac{F'}{\eta} \left(1 - \frac{F'}{\eta}\right) \eta d\eta + \beta \int_0^{\infty} \left[1 - \left(\frac{F'}{\eta}\right)^2\right] \eta d\eta = 0 \quad (11)$$

Approximate solutions are derived by assuming

$$F'/\eta = 1 + [(F'/\eta)_0 - 1]e^{-b\eta^{2/4}} \quad (12)$$

where $(F'/\eta)_0$ and b are constants. $(F'/\eta)_0$ is determined by satisfying Eq. (11), and b by evaluating Eq. (1a) at $\eta = 0$. There results

$$(F'/\eta)_0 = -[(1 + 3\beta)/(1 + \beta)] \quad b = 2\beta^2/(1 + \beta)$$

Furthermore, the following exact result can be derived from Eq. (11): $\delta^*/\theta = -[(1 + \beta)/\beta]$; where δ^* and θ are, respectively, the displacement and momentum thicknesses.

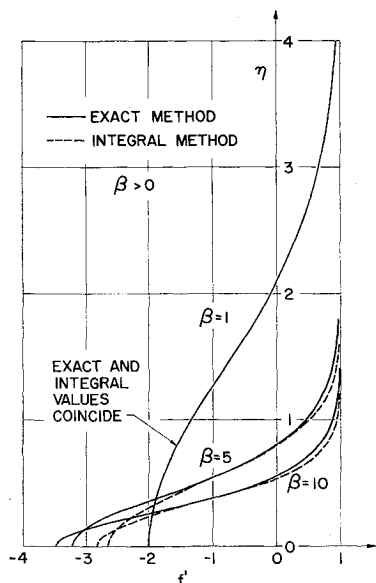


Fig. 3 Velocity profiles for $\beta > 0.5$.

The pertinent results are presented in Table 1 and Figs. 1-3. The exact results in the range $-0.5 < \beta < 0$ have been taken from Ref. 3. The new results presented here show that for $-1.0 < \beta < -0.5$ the F'/η profiles are monotonic and jet-like, whereas in the range $0.5 < \beta < \infty$ the F'/η profiles are monotonic and wake-like. The possibility of deriving solutions when $0 < \beta < 0.5$ is now being investigated.

References

- ¹Steiger, M. H. and Bloom, M. H., "Linearized viscous free mixing with streamwise pressure gradients," AIAA J. 2, 263-266 (1964).
- ²Steiger, M. H., "Similarity in axisymmetric viscous free mixing with streamwise pressure gradient," AIAA J. 2, 1509-1510 (1964).
- ³Kubota, T., Reeves, B., and Buss, H., "A family of similar solutions for axisymmetric incompressible wakes," AIAA J. 2, 1493-1495 (1964).
- ⁴Steiger, M. H. and Chen, K., "Further similarity solutions of two-dimensional wakes and jets," Polytechnic Institute of Brooklyn, PIBAL Rept. 811 (August 1964).

Wave Intersection Limits for Focused Compression of Air in Chemical Equilibrium

LOWELL W. PEARSON* AND FRANCIS J. SCHOELLEN†
North American Aviation, Inc., Los Angeles, Calif.

INLETS for hypersonic ramjets^{1, 2} using isentropic, external compression have attractive weight-saving features. These inlets, at their design points, require that the compression-surface-generated, one-family characteristics be focused near the cowl leading edge to minimize spillage drag. The first design consideration should be the flow-turning limitations imposed by the shock structure at the focal point. It is the purpose of this paper to present these limitations as calculated for equilibrium air to Mach number 8 for two-dimensional flow. A comparison of these results with an extension of the work by Connors and Meyer³ for a perfect gas is also presented.

As stated in Ref. 3, the limiting amount of isentropic flow turning with focused characteristics is determined from analysis of the branch-shock configuration, which consists of a single intersection of an isentropic compression fan, a reflected wave, a vortex sheet, and shock wave (Fig. 1). Theoretical requirements of any wave intersection are that equal static pressures and flow direction exist on either side of the

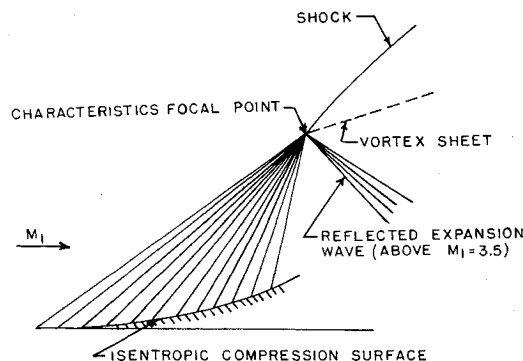


Fig. 1 Schematic of the branch-shock structure analyzed for maximum isentropic compressive turning.

Received September 23, 1964.

* Senior Engineer, Aerodynamics. Member AIAA

† Senior Engineer, Aerodynamics.